
Flow Separation Control Over a Ramp with Nanosecond-Pulsed Plasma Actuators

Y.D. Cui, Z.J. Zhao, J. Li, J.G. Zheng, and B.C. Khoo

Introduction

Flow separation control using alternating current dielectric barrier discharge (AC-DBD) plasma actuators has been widely studied [1–4]. These devices have some unique advantages, such as no mechanical parts, low power consumption, fast response time and high-frequency broadband. Typically, the DBD plasma actuator consists of two electrodes separated by a thin dielectric layer and is driven by high AC voltage with frequencies ranging from kilohertz to a few tens of kilohertz. The dominant mechanism of AC-DBD actuators on flow control is relevant to the momentum transfer due to the colliding particles [electrohydrodynamic effect (EHD)], forming an induced surface wall jet. One of the most critical issues of AC-DBD plasma flow control technology is its saturation of space charge densities and electric field in the plasma discharge, limiting its application in low speed regime [2].

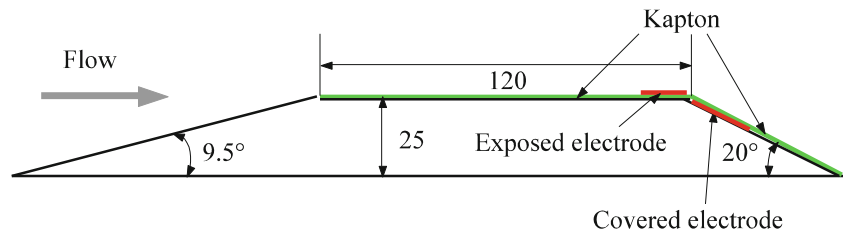
Recently, much attention has been put into nanosecond-pulsed dielectric barrier discharge (ns-DBD) plasma actuators. This type of actuator usually has similar configurations as the AC-DBD device, but it is driven by a train of high-voltage pulses with each pulse rise and decay time at several to tens of nanoseconds. Several studies have examined the applicability of the ns-DBD plasma actuators to flow control under both subsonic and supersonic flow conditions [5–7]. It has been generally agreed that the main control mechanism of the ns-DBD plasma actuator is through Joule heating, which is different from the AC-DBD by momentum adding from the induced ionic wind. Joule heating causes steep gradients in pressure and temperature inside the heated gas volume. As a result, moving shock waves are generated and interact with the external flow.

While the previous studies have focused on the effectiveness of the actuators on specific applications, how the generated shock waves influence and interact with the external flow has not been thoroughly investigated. The very recent experimental and numerical studies in quiescent air by Zhao et al. [8] and Zheng et al. [9] revealed that the shock wave is basically a kind of micro-blast wave. It was observed that the blast wave can be fairly strong in terms of the induced fluid velocity (of up to hundreds m/s) and the overpressure (of up to tens of kPas) shortly after its initiation but decays very fast. It was also noted that the shock-induced perturbations (overpressure and induced velocity) are restricted to a narrow region behind the blast wave front, lasting for a few microseconds only, showing extremely localized effects in space and transient effects in time [8, 9]. In the recent experimental work by Correale et al. [10], the residual heat, however, was reported to be able to trigger natural flow instabilities, which can be essential for controlling certain flows.

To better understand how the perturbations caused by the nanosecond-pulsed plasma affect the separated flow, this paper is to study the process of suppressing the separated flow over a ramp (Fig. 1) with nanosecond-pulsed plasma actuators in a wind tunnel. A ramp was chosen as a study case as its geometry is simple and has fixed separation point at the corner of the downstream deceleration ramp, compared to the changing separation point with Reynolds number over an airfoil. The downstream deceleration ramp can also be changed to various configurations, such as backward-facing step (BFS) when the angle of the ramp equals to 90° . A recent study using AC-DBD to control the flow downstream of a BFS [11] made a good summary on the flow behaviours. Their results showed that the best location to reduce the flow recirculation is immediately upstream of the separation, before the instabilities take place, and the forcing frequency within the range of the natural shedding frequency leads to drastic changes in the time-averaged turbulent flow field presumably due to a lock-on effect, which is consistent

Y.D. Cui (✉) • Z.J. Zhao • J. Li • J.G. Zheng • B.C. Khoo
Temasek Laboratories, National University of Singapore,
5A Engineering Drive 1, Singapore 117411, Singapore
e-mail: tslycd@nus.edu.sg

Fig. 1 Sketch of the ramp model with DBD actuators



with the study by Hasan [12]. Correale et al. [13] investigated the effects of ns-DBD on the BFS flow at Re of 3600 based on the step height. Their results showed the reattachment length reach reaches a minimum of about 60 % of the non-actuated case at a frequency of 140 Hz, which is close to the natural frequencies of the Kelvin-Helmholtz instability. However, how the nanosecond-pulsed plasma actuators affect the separated flow was not given.

The present study is attempted to examine how the actuation of the pulsed plasma affects the separated flow downstream of a deceleration ramp by experiments with smoke-wire visualization and particle image velocimetry (PIV). The experiments were performed in a small-scale blowdown low speed wind tunnel located at Temasek Laboratories of the National University of Singapore. This wind tunnel has a contraction ratio of 9.8 and a test section of $0.16 \text{ m} \times 0.16 \text{ m}$ with turbulence intensity level less than 0.25 % and maximum speed of 30 m/s. The test section has a length of 0.75 m and was made from Perspex to facilitate flow visualizations and PIV measurements. The ramp configuration follows the dimensions of Ref. [14] as shown in Fig. 1. The ns-DBD plasma actuator comprises two electrodes (copper foil with a thickness of $66 \mu\text{m}$) mounted on both sides of a dielectric layer. This dielectric layer is made of four layers of Kapton films (Kapton 500FN131, $175 \mu\text{m}$ thick) and covers the whole plateau and downstream ramp. The widths of the exposed and the encapsulated electrodes are 8 and 15 mm, respectively. The connection point between the two electrodes is located at 1 mm upstream of the turning point of the ramp with a gap of about 0–0.1 mm.

The nanosecond pulse to drive the ns-DBD plasma actuator was achieved by means of a nanosecond pulse generator (NPG-18/3500). This generator produces high-voltage pulses with the peak voltage from 12 to 20 kV at matched 75Ω load, the pulse rise time of about 4 ns, the repetition rate of up to 3.5 kHz and the energy of up to 30 mJ/pulse. Note that the peak voltage, the current and the associated energy are strongly load dependent. The applied voltage and current were measured using a high-voltage probe (Tektronix P6015A) and a current shunt probe (Megaimpulse CS-10/500), respectively. The current probe has an internal impedance of 0.2Ω and a time resolution of 1 ns. In order to apply this probe to measure a pulse with nanosecond rise times, a calibration was conducted using a square wave (30Vp-p) with a rise time of ≤ 10 ns and with a duration of 100 ns (generated from digital delay generator model DG645) following the manual of Tektronix P6015A.

Flow visualization at low speed regime (3 m/s) was conducted with smoke-wire technique. An in-house smoke-wire system was used in this study. It consists of a container holding paraffin oil having a needle outlet (inside a diameter about 0.6 mm) and was mounted on the top of the test section. A resistance heating wire (nickel-chromium alloy) diameter of 0.193 mm passed from the needle and through the test section vertically. The paraffin oil dropped along the wire. When the wire is heated by a DC power supply, the oil can be evaporated and form very fine smoke filaments. To obtain high-quality images, a LED light was used to illuminate the flow field, and the images were captured using a high-speed camera (Photron FastCAM SA-Z, 1024×1024 pixels, 12 bit). This camera is able to acquire at 20 kHz at full-frame resolution and at 100 kHz at 640×280 pixels.

Flow field at high-speed regime (30 m/s) was measured using a two-velocity component particle image velocimetry (PIV) system (DANTEC) with a pulsed Nd:YAG laser forming a pair of thin light sheets. The time between two image frames used for particle scattering was set according to the flow velocity, the camera magnification and the sub-region area for cross-correlation. A pair of images was acquired by the PCO 2000 camera (2048×2048 pixel) with the Nikon Nikkor microlens (105 mm $f1:2.8D$). For each image, 32×32 pixels of subregion area with 50 % overlap were adopted in performing the cross-correlation. The resulting velocity fields were further post-processed to remove spurious vectors by using the range validation function. A smoke generator was used to provide particles of a mean diameter of 2–5 μm . A DG645 digital delay generator was used to precisely synchronize the nanosecond pulse generator, high-speed camera and/or the PIV system.

Results

The measured voltage and current waveforms over the actuator used in this experiment are shown in Fig. 2. The peak voltage and current are approximately 24 kV and 140A, respectively. The corresponding peak power is calculated about 3200 kW. The duration time of full width at half maximum (FWHM) is about 14 ns.

Figure 3 shows smoke-wire visualization results over the downstream ramp (20°) using high-speed camera (500 frame/s) at the freestream velocity $U = 3$ m/s, with the actuation frequency of 3 kHz. A large separation was obvious when the actuator was off (Fig. 3a).

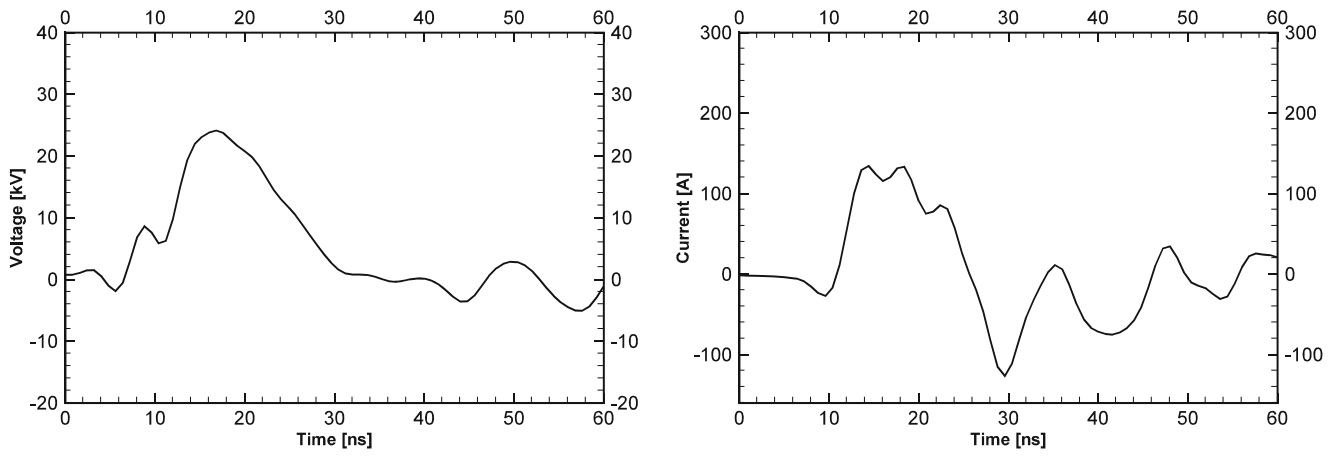


Fig. 2 Measured voltages and current acting on the actuator

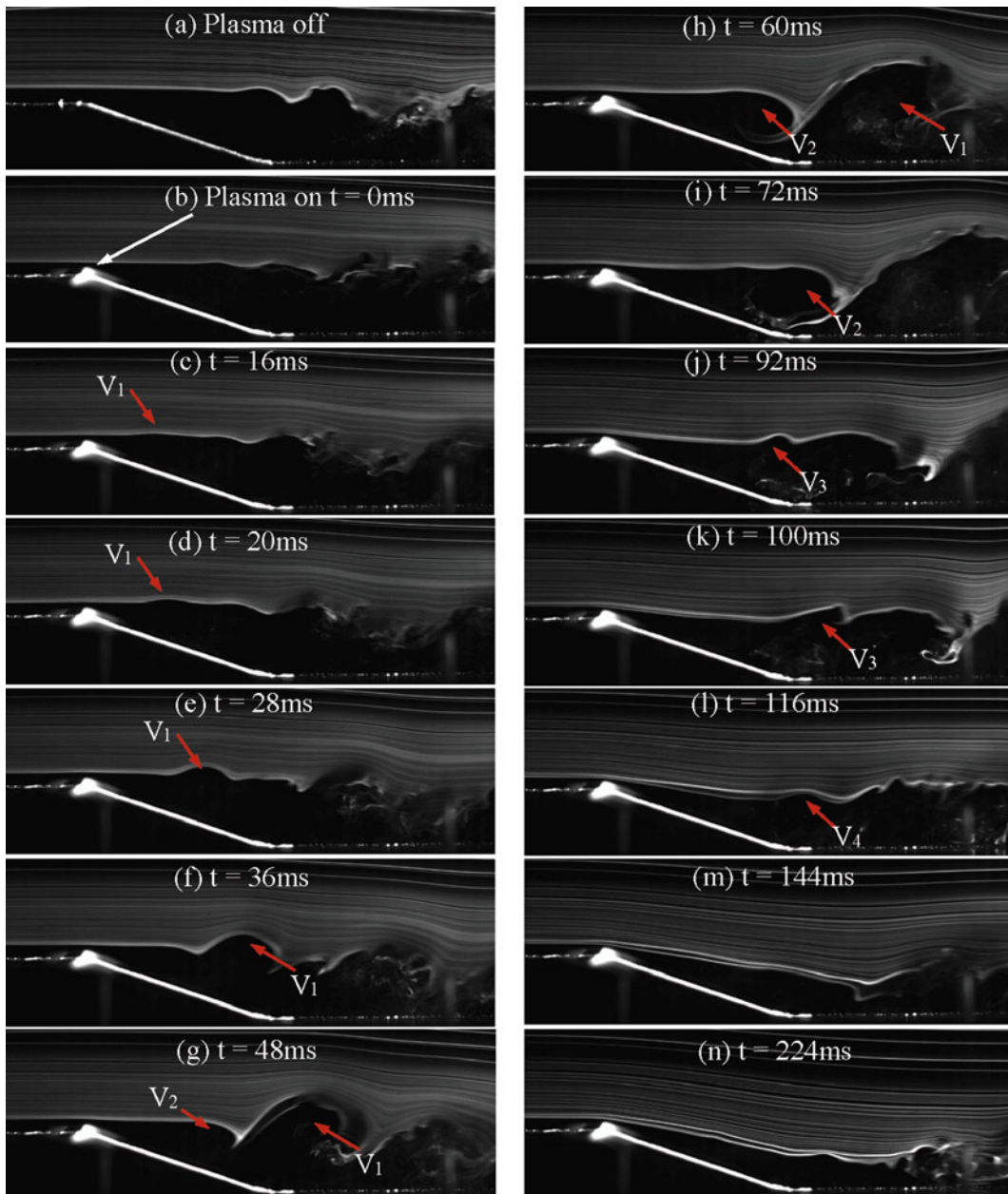


Fig. 3 Smoke-wire visualization results at $U = 3$ m/s using high-speed camera

When the actuator is on, it can be seen clearly that the smoke filaments changed dramatically to a quasi-attached flow over the ramp. In the process of flow reattachment, a series of vortices play an important role. At $t = 28$ ms, it can be observed that the smoke filament bumped up indicating that a vortex (termed as V_1) was formed. As this vortex moved downstream, another vortex (V_2) was formed (Fig. 3f, g). Again, a third vortex (V_3) was formed as V_2 moved downstream. Following this process, the flow (smoke filaments) was reattached to the downstream ramp. Note that there are still series of small-scale vortices which was formed and moved downstream even in the quasi-attached flow (Fig. 3n).

Figure 4 presents typical PIV measurement results using phase-locked technique at the same conditions as of Fig. 3. It is evident that a series of vortices were formed in the earlier stage of the actuation of plasma actuator (Fig. 4b, c), and the flow was almost attached to the ramp in the final stage but with small-scale vortices close to the ramp surface. At higher freestream velocity of 30 m/s, as smoke-wire technique was not working, only PIV measurement was attempted. Note that there was no obvious flow separation over the ramp at this condition; a ramp with 45° was used for PIV measurement as shown in Fig. 5. Though the flow was not fully attached to the ramp surface, the effectiveness of the pulsed plasma actuation is observed.

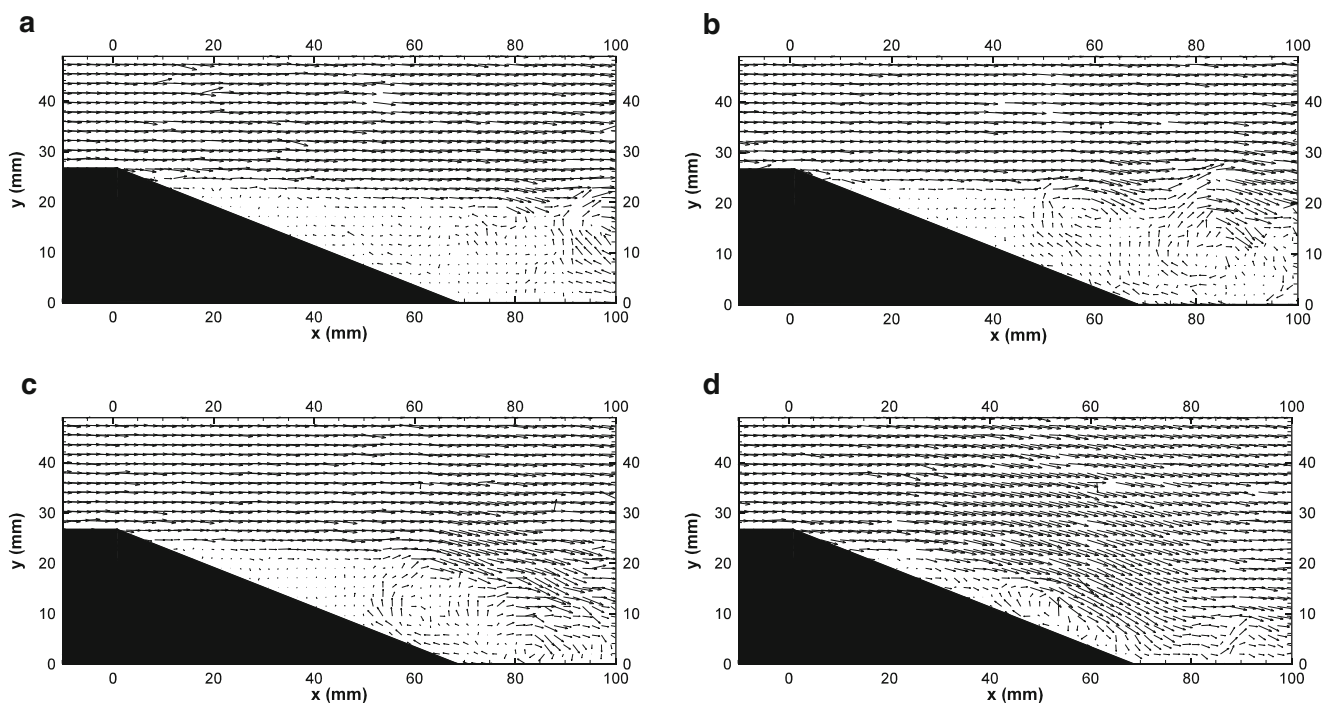


Fig. 4 Flow field measurement using PIV at $U = 3$ m/s. (a) Plasma off. (b) Plasma on $t = 15$ ms. (c) Plasma on $t = 19$ ms. (d) Plasma on $t = 1$ s

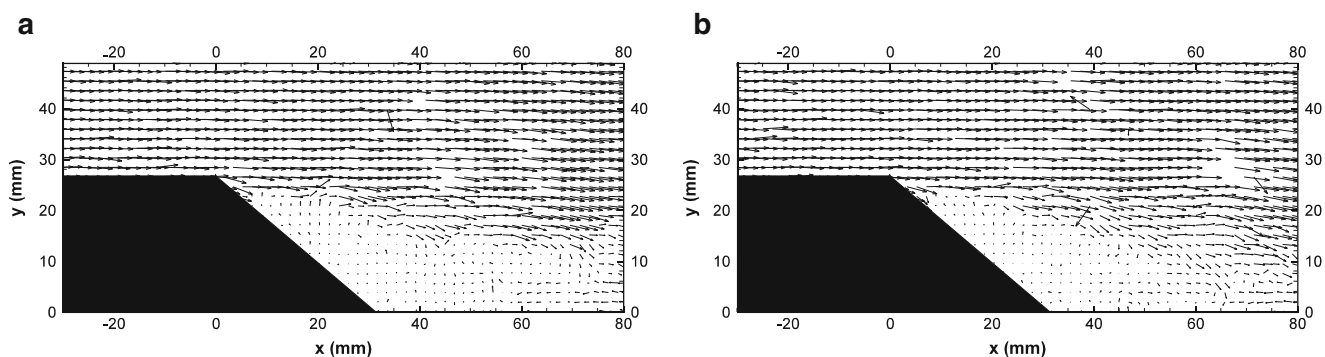


Fig. 5 Flow field measurement using PIV at $U = 30$ m/s for the ramp of 45° . (a) Plasma off. (b) Plasma on $t = 1$ s

Conclusions

In this paper, we studied the effects of nanosecond-pulsed plasma actuators on the separated flow over a ramp in a wind tunnel using smoke-wire technique with high-speed camera and PIV measurements. The results indicate that a series of vortices were generated along the shear layer of the separated flow over the deceleration ramp. These vortices could be formed by the interactions between the shear layer of the separated flow and the perturbations (induced velocities) caused by the blast waves generated by the pulsed plasma. It appears that these vortices draw external flow energy resulting in the separated flow attached to the ramp surface.

References

- Moreau, E.: Airflow control by non-thermal plasma actuators. *J. Phys. D Appl. Phys.* **40**(2007), 605–636 (2007)
- Forte, M., Jolibois, J., Pons, J., Moreau, E., Touchard, G., Cazalens, M.: Optimization of a dielectric barrier discharge actuator by stationary and non-stationary measurements of the induced flow velocity application to airflow control. *Exp. Fluid.* **43**, 917–928 (2007)
- Thomas, F., Corke, T., Igbal, M., Kozlov, A., Schatzman, D.: Optimization of dielectric barrier discharge plasma actuators for active aerodynamic flow control. *AIAA J.* **47**(9), 2169–2178 (2009)
- Corke, T.C., Enloe, C., Wilkinson, S.P.: Dielectric barrier discharge plasma actuators for flow control. *Annu. Rev. Fluid Mech.* **42**, 505–529 (2010)
- Roupassov, D., Nikipelov, A., Nudnova, M., Starikovskii, A.: Flow separation control by plasma actuator with nanosecond pulsed-periodic discharge. *AIAA J.* **47**(1), 168–185 (2009)
- Starikovskii, A., Nikipelov, A., Nudnova, M., Roupassov, D.: SDBD plasma actuator with nanosecond pulse-periodic discharge. *Plasma Sources Sci. Technol.* **18**, 034015 (2009)
- Little, J., Takashima, K., Nishihara, M., Adamovich, I., Samimy, M.: Separation control with nanosecond-pulse-driven dielectric barrier discharge plasma actuators. *AIAA J.* **50**(2), 350–365 (2012)
- Zhao, Z.J., Li, J., Zheng, J.G., Cui, Y.D., Khoo, B.C.: Study of shock and induced flow dynamics by pulsed nanosecond DBD plasma actuators. *AIAA J.* **53**(5), 1336–1348 (2015)
- Zheng, J.G., Zhao, Z.J., Li, J., Cui, Y.D., Khoo, B.C.: Numerical simulation of nanosecond pulsed dielectric barrier discharge actuator in a quiescent flow. *Phys. Fluid.* **26**, 036102 (2014)
- Correale, G., Michelis, T., Ragni, D., Kotsonis, M., Scarano, F.: Nanosecond pulsed plasma actuation in quiescent air and laminar boundary layer. *J. Phys. D Appl. Phys.* **47**, 105201 (2014)
- Sujar-Garrido, P., Bernard, N., Moreau, E., Bonnet, J.P.: Dielectric barrier discharge plasma actuator to control turbulent flow downstream of a backward-facing step. *Exp. Fluid.* **56**(4) (2015)
- Hasan, M.: The flow over a backward-facing step under controlled perturbation: laminar separation. *J. Fluid Mech.* **238**, 73–96 (1992)
- Correale, G., Michelis, T., Kotsonis, M.: NS-DBD plasma actuation on a backward facing step. *AIAA Paper AIAA 2014-0325*, 13–17 January 2014, National Harbor, MD, 52nd Aerospace Science Meeting, (2014)
- Caruana, D., Rogier, F., Dufour, G., Gleyzes, C.: The plasma synthetic jet actuator, physics, modeling and flow control application on separation. *J. Aerospace Lab., Onera*, (6) (2013)